# Dependency of Heterojunction Transistors' Speed on Various Physical Parameters: A Comparative Study of SiGe & AlGaAs HBTs

Priyanka Biswas, Rowshon Ara Mannan[#], Nusrat Jahan
Dept. of Electrical, Electron & Communication Engineering
Military Institute of Science and Technology (MIST)
Mirpur, Dhaka, Bangladesh
[#]munneehcc09@yahoo.com

Yeasir Arafat[*]
Department of Electrical and Electronic Engineering
Bangladesh University of Engineering and Tech. (BUET)
Dhaka, Bangladesh
[*]arafat@eee.buet.ac.bd

***Abstract*—It is very essential to find out how the speed of a Heterojunction Bipolar Transistor (HBT) depends on different physical parameters of the transistor as the device has become indispensable in modern ultrafast circuits. As the speed of an HBT is a very strong function of its base transit time, here we investigate its dependency on minority carrier injection, base width, base emitter voltage, peak base doping concentration and slope of base doping for an $AlGaAs$ HBT. The analytical model of base transit time of this $AlGaAs$ HBT is based on $SiGe$ model as found in literature. Comparison of base transit time obtained from similar simulation for $SiGe$ and $AlGaAs$ HBT has been presented in this work.**

***Keywords—Comparison of base transit time; HBT; Gaussian doping profile; Minority carrier injection.***

## I. INTRODUCTION

The high speed application of heterojunction bipolar transistor has increased its use in electronics extensively now-a- days. Heterojunction bipolar transistors have many other advantages over its homojunction bipolar counterparts. Recent work shows that this technology is being used to develop electronics for space applications because of their excellent analog and radio frequency (RF) performance over an extremely wide range of temperatures [1]. $SiGe$ HBTs have been introduced as the technology of choice for RF integrated circuits due to its high speed performance and mature silicon process [2]. $GaAs-AlGaAs$ HBT process technology is reported to be used in the fabrication of large number of complex analog integrated circuits for commercial and military applications [3].

The speed of a junction transistor is dependent on the transit time of an electron through the transistor. The transit time has three components-emitter transit time, base transit time and collector transit time. Since base transit time contributes to more than 70% of the junction transistor's total transit time [4] its speed is mainly determined by the factors which affects the base transit time of the device. The base transit time of a heterojunction bipolar transistor is influenced by many physical and electrical parameters and various other factors. These factors include base width, various doping concentration profiles in the base region (uniform, exponential, Gaussian), various alloy material profiles in the base region (box, triangular, and trapezoidal), velocity saturation effect, collector current density, built-in electric field in the base region, electric field and doping dependent carrier mobility, bandgap narrowing and base resistance. In this paper we investigate the effect of some of these parameters on the base transit time and hence speed of an $AlGaAs$ HBT. Finally a comparison of the base transit time for a $SiGe$ HBT and $AlGaAs$ HBT has been done.

## II. ANALYSIS

The $Al$ mole fraction $(y)$ distribution profiles of an *n-p-n* $Al_yGa_{1-y}As$ base HBT can mathematically be represented as shown in (1). In general, the trapezoidal profile of $y$ can be expressed as a function of distance $(x)$ along the neutral base width $W_B$, as

$$y(x) = m_{Al}x + y_E \tag{1}$$

where, $m_{Al} = y_C - y_E/W_B$; $y_C$ and $y_E$ are $Al$ fraction at the collector and emitter end respectively. For $y_E$=0, (1) represents triangular profile; for $y_E$=$y_C$, (1) represents box shape profile [5].

Total $Al$ content within the base is called $Al$ dose and is calculated as [6]

$$y_D = y_{av}W_B \tag{2}$$

$$\text{where,}\quad y_{av} = (y_C + y_E)/2 \tag{3}$$

The base transit time of a HBT can be expressed as [7]

$$\tau_B = q\int_0^{W_B}\frac{n(x)}{J_n(x)}dx \tag{4}$$

where, $n(x)$ is the minority carrier concentration and $J_n(x)$ is the electron current density within the base, $q$ is the charge of an electron. For the base region, $n(x)$ can be found using the transport equations and electric field equations as given respectively below [8].

$$-J_n = qD_n(x)\frac{dn(x)}{dx} + q\mu_n(x)E(x)n(x) \quad (5a)$$

$$J_p = -qD_p(x)\frac{dp(x)}{dx} + q\mu_p(x)E(x)p(x) \quad (5b)$$

and

$$E(x) = \frac{kT}{q}\left(\frac{1}{p(x)}\frac{dp(x)}{dx} - \frac{1}{n_{ie}^2(x)}\frac{dn_{ie}^2(x)}{dx}\right) \quad (6)$$

where, $D_n(x)$ and $D_p(x)$ are the electron and hole diffusivity, $\mu_n(x)$ and $\mu_p(x)$ are electron and hole mobility respectively. $E(x)$ is the electric field, $p(x)$ is the hole concentration and $n_{ie}(x)$ is the effective intrinsic carrier concentration. $J_n$ in (5a) is defined such that it has a positive value. As the base width of today's high-speed HBT is less than 100 nm even 26 nm base width is used in literature [6], so the carrier recombination in the base region can safely be neglected, resulting in $J_p$ in (5b) approximately zero and a constant $J_n$ which finally equals to the collector current$J_c$. In entire derivation, the minority carrier concentration at thermal equilibrium has been neglected. Neglecting $J_p$ and using (5a), (6) along with Einstein's relation $D_n(x) = V_T\mu_n(x)$, the total current density becomes

$$-J_n = qD_n(x)\frac{n_{ie}^2(x)}{n(x)+N_B(x)}\frac{d}{dx}\left[\frac{n(x)\{n(x)+N_B(x)\}}{n_{ie}^2(x)}\right] \quad (7)$$

where, $N_B(x)$ is the base doping concentration. Doping profile used in this analysis is Gaussian and given by [9]

$$N_B(x) = N_B(0)\exp(-mx^2) \quad (8)$$

where, $N_B(0)$ is the peak base doping concentration; $m = \frac{1}{2\sigma^2}$ and $\sigma = W_B/\sqrt{2\ln\frac{N_B(0)}{N_B(W_B)}}$.

The low field doping density dependent electron diffusivity in $GaAs$ can be written as [10]

$$D_{nGaAs}(x) = D_n\exp(m_1x^2) \quad (9a)$$

where, $D_{nl} = D_{n0}(N_B(0)/N_r)^{-\gamma_1}$;$D_{n0} = 207\ cm^2/s$[11]; $m_1 = m\gamma_1$; $\gamma_1 = 0.42$; $N_r = 10^{17}cm^{-3}$.

Now, in the presence of $Al$, the electron diffusivity will be changed as [12]

$$D_{nAlGaAs}(x) = bD_{nGaAs}(x) \quad (9b)$$

where, $b = 1 + 3y_{av}$.The saturation velocity inside the $AlGaAs$ alloy also differs from that in $GaAs$. It is given by [13]

$$v_{sA} = cv_s \quad (10)$$

where, $c = 0.342/[0.342 + y_{av}(1 + y_{av})]$; $v_S = 7 \times 10^6\ cm/s$[14].

The effective intrinsic concentration in $AlGaAs$ is [12]

$$n_{ieAlGaAs}^2(x) = n_{ioGaAs}^2\gamma_r e^{\frac{\Delta E_{geff}(x)}{kT}} \quad (11a)$$

where, $\gamma_r$ is the ratio of the effective DOS in $AlGaAs$ base to the effective DOS in $GaAs$ and given by [15], [16]

$$\gamma_r = \exp\left(-\sqrt{5y_{av}}\right) \quad (11b)$$

$n_{ioGaAs} = 2.1 \times 10^6 cm^{-3}$, is the intrinsic carrier concentration in undoped $GaAs$ [14]; $k$ is the Boltzmann constant; $T$ is the temperature in degrees Kelvin; $E_{geff}(x)$ is the effective bandgap reduction in the $GaAs$ base that can be expressed as

$$E_{geff}(x) = \Delta E_{gHD}(x) + \Delta E_{gAl}(x) \quad (11c)$$

where $\Delta E_{gAl}(x)$ is the BGN due to the presence of which is assumed to have a linear dependency on $Al$ fraction; $\Delta E_{gHD}(x)$ is the BGN due to heavy doping effects and is identical to that of $GaAs$ [15]. An approximation of the Slotboom–de Graff BGN model [17] is used for this term [18]

$$\Delta E_{gHD}(x) = qV_{gHD}\ln\left(\frac{N_B(x)}{N_r}\right) \quad (11d)$$

with, $V_{gHD}$= 0.0229V and the BGN due to the presence of $Al$ is given by [19]

$$\Delta E_{gAl}(x) = qV_{gAl}y(x) \quad (11e)$$

with, $V_{gAl}$= $10^{-10}$ V

Rearranging (11a)-(11e), effective intrinsic concentration in $AlGaAs$ can be expressed as

$$n_{ieAlGaAs}^2(x) = n_{ieAlGaAs}^2(0)\exp(m_3x - m_2x^2) \quad (12)$$

where, $n_{ieAlGaAs}^2(0) = n_{ioSi}^2\gamma_r\exp(\gamma_3y_E)\left(\frac{N_B(0)}{N_r}\right)^{\gamma_2}$;$\gamma_2 = V_{gHD}/V_T$; $\gamma_3 = V_{gAl}/V_T$; $V_T = kT/q$; $m_2 = m\gamma_2$; $m_3 = m_{Al}\gamma_3$.

For low injection, $n(x) \ll N_B(x)$ and the quasi-neutral condition becomes [20]

$$p(x) = N_B(x) \quad (13)$$

Putting it in (6) and replacing the $GaAs$ terms by $AlGaAs$ terms, $E(x)$ for low injection can be written as

$$E_{lAlGaAs}(x) = -V_T(m_3 + m_4x) \quad (14)$$

where, $m_4 = 2(m - m_2)$. Similarly, replacing the $GaAs$ terms by $AlGaAs$ terms in (7), $J_{nl}$ (for low injection) can be written as

$$-J_{nl} = qD_{nAlGaAs}(x)\frac{n_{ieAlGaAs}^2(x)}{N_B(x)}\frac{d}{dx}\left[\frac{n_l(x)N_B(x)}{n_{ieAlGaAs}^2(x)}\right] \quad (15)$$

Using the equation for $n_{ieAlGaAs}^2(x)$, $N_B(x)$ and $D_{nAlGaAs}(x)$ in (15), differential equation for minority carrier concentration $n_l(x)$ can be solved for $n_l(x)$ as [21]

$$n_l(x) = exp\left(m_4\frac{x^2}{2} + m_3x\right)\left(n_l(0) - J_{nl}(B_1(x) + B_2(x) + B_3(x))\right) \quad (16)$$

At $x = 0$, the electron concentration can be found by using [22] with necessary correction for $AlGaAs$

$$n_l(0) = \frac{n_{ieAlGaAs}^2(0)}{N_B(0)}\exp\left(\frac{V_{be}}{V_T}\right)f_w \quad (17)$$

where, $f_w = \frac{1}{0.5+\sqrt{0.25+\frac{n_{ieAlGaAs}^2(0)}{N_B(0)}\exp\left(\frac{V_{be}}{V_T}\right)}}$ (17a)

Though Suzuki used this initial condition for high injection region considering Webster effect [23], it is also valid for low injection [20], as the value of $f_w$ becomes unity for $V_{be} \leq 1.1\ V$.

Putting x=$W_B$ in (16), the electron concentration $n(W_B)$ becomes

$$n_l(W_B) = \frac{n_l(0)exp\left(m_4\frac{W_B^2}{2}+m_3W_B\right)}{1+qv_{sA}exp\left(m_4\frac{W_B^2}{2}+m_3W_B\right)(B_1(W_B)+B_2(W_B)+B_3(W_B))} \quad (18)$$

Assuming that the electron velocity in the base collector depletion region saturates at $v_{sA}$, the electron current density $J_{nl}$ at x=$W_B$ can be given by

$$J_{nl} = qv_{sA}n_l(W_B) \quad (19)$$

The base stored charge per unit area is given by

$$Q_{Bnl} = q\int_0^{W_B} n_l\,(x)dx \quad (20)$$

Using (19) and (20), the base transit time equation for low injection (4) becomes $\tau_{Bl} = \frac{Q_{Bnl}}{J_{nl}}$ (20a)

The modified carrier concentration and current density for moderate injection can be given by,

$$n_m(x) = f_W n_l(x) \quad (21)$$

$$J_{nm} = f_W J_{nl} \quad (22)$$

Here $f_w$ is used to incorporate Webster effect. Assuming that the injected electron concentration is perturbed by the modulated electric field from $n_m(x)$ only a little and also using quasi-neutrality of charge equation, we can find $n(x)$ and $p(x)$ for moderate injection as below,

$$n(x) = n_m(x) + \delta n(x) \quad (23)$$

$$p(x) = n_m(x) + \delta n(x) + N_B(x) = p_m(x) + \delta n(x) \quad (24)$$

Now, following the same procedure as low injections and using equations (8), (9a), (12), (21-24), we can solve (15) to find $n(x)$ for moderate injection, [9]

$$n(x) = \frac{\exp(m_3x - m_2x^2)}{p_m(x)}\left(n(0)p_m(0) + \frac{J_n}{qv_{sA}}N(x)\right) \quad (25)$$

Putting $x$=$W_B$ in equation (25), we can find $n(W_B)$ and hence calculate $J_n$ for moderate injection with similar equation as (19). Finally total stored base charge and base transit time can be calculated following equations (20) and (4).

## III. RESULT

Distribution of injected electron concentration $n(x)$ within the base for three different $Al$ profiles at a given base doping slope & peak base doping $N_B(0)$ is shown in Figure 1 for low injection. From Figure 1 it is observed that $n(x)$ for box $Al$ profile is lower than that of trapezoidal $Al$ profile and for triangular profile, $n(x)$ remains above all other distributions. This is because the transport of electron through the base is assisted by the gradient in $Al$ profiles [24]. The gradient is highest for triangular profile, zero for box profile and in-between for trapezoidal profile (referred to Figure 1). So for triangular $Al$ profile, electron passes slower through the base to enter the collector and distribution of $n(x)$ remains higher.

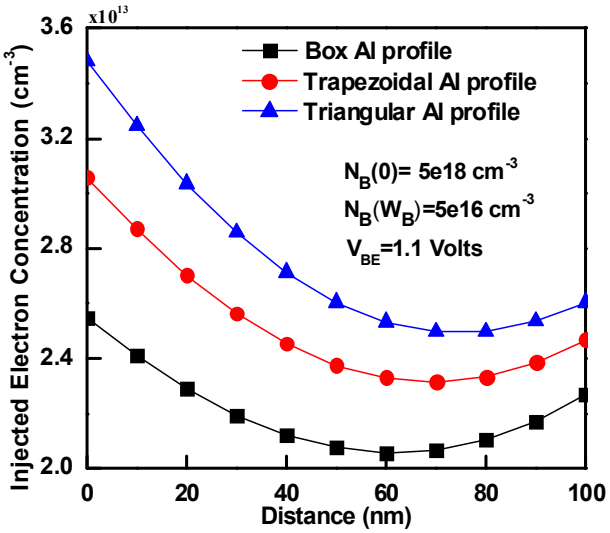


Fig. 1. Injected electron distribution within the base for box $Al$ profile ($y_C$=0.25, $y_E$=0.2499) under low ($v_{be}$=1.1) level of injection.

Dependence of normalized injected electron distribution on base width ($W_B$) is shown in Figure 2. From this plot it is evident that as $W_B$ decreases, $n(x)/n(0)$ increases. This happens because for shorter base, injected minority carriers get relatively small time to be diffused compared to longer base. So (n($W_B$))/(n(0)) for longer base is lower than that of a shorter base. The injected electron concentration profiles shown in Figure 1 is not linear due to the built in electric field caused by the Gaussian base doping and the gradient in $Al$ profile. It is also found that the minority carrier has maximum value at the base-emitter junction and minimum value at the collector-base junction. It decreases from its peak value as the distance from the emitter increases. In this work velocity saturation of electron at the collector-base junction is considered. So at collector-base junction the minority carrier concentrations for low and high levels of injection are not zero.

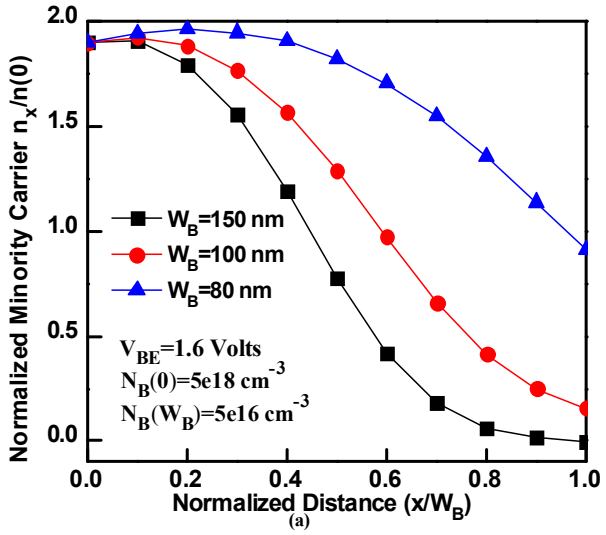


Fig. 2. Normalized minority carrier electron distribution within the base for different base widths with trapezoidal *Al* profile $y_C$=0.25, $y_E$=0.1

Variation of minority carrier injection ratio $n(0)/N_B\ (0)$ with $V_{be}$ at a given $N_B\ (0)$, slope of base doping and $W_B$ is shown in Figure 3. The figure shows that $n(0)/N_B\ (0)$ is an increasing function of $V_{be}$. From equation (17) it is found that n(0) is exponentially proportional to $V_{be}$. So, for a given $N_B\ (0)$, minority carrier injection ratio will also increase exponentially with $V_{be}$ but under moderate injection the exponential slope will decrease due to Kirk effect at a certain high current [6]. For this reason, the low injection part of Figure 3 (which is a logarithmic plot) is linear and at the beginning of high injection, its slope starts to fall.

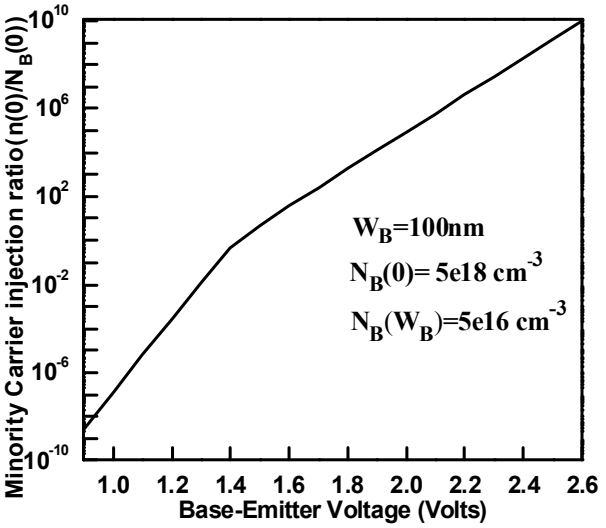


Fig. 3. Minority carrier injection ratio as a function of base emitter voltage

As discussed earlier in Figure 3, minority carrier injection ratio is an increasing function of base-emitter voltage. So, the variation of the base transit time with the minority carrier injection ratio has the same pattern as the base transit time varies with base-emitter voltage shown in Figure 4. The variation of base transit time with the minority carrier injection ratio, the aiding field reduces, electron slows down and base transit time increases.

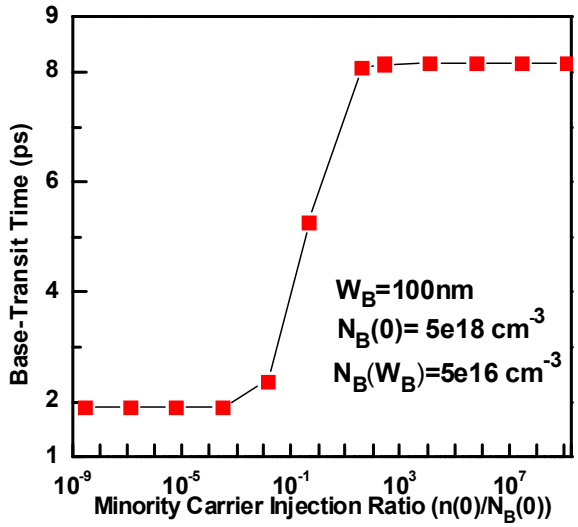


Fig. 4. Base transit time as a function of minority carrier injection ratio for box shape *Al* profile (Box: $y_C$=0.25, $y_E$=0.2499)(considering doping dependent mobility).

The dependence of base transit time ($\tau_B$) upon base width ($W_B$) at a given base profile is shown in Figure 5. From this figures it is clear that $\tau_B$ is an increasing function of $W_B$ as was found in the mathematical analysis. With the increase in $W_B$, the stored base charge increases and $n(W_B)$ decreases (shown in Figure 2): this results in a reduction in electron current density as defined by equation (19), eventually the base transit time experiences two fold increase as per (20a).

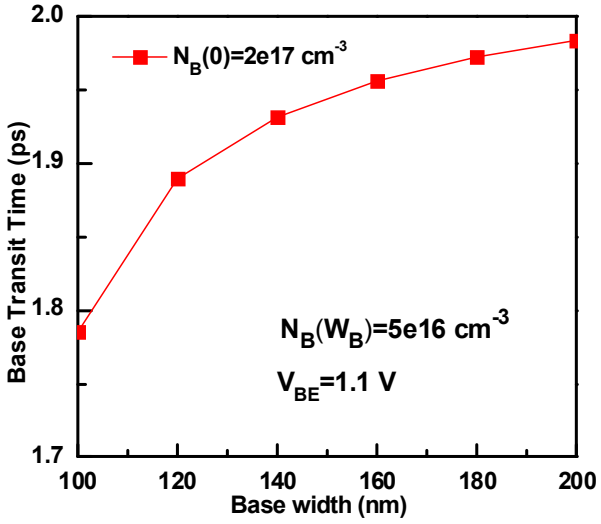


Fig. 5. Base transit time as function of base width for lightly doped base with trapezoidal *Al* profile (Trapezoidal: $y_C$=0=0.25, $y_E$=0.1)

The dependence of base transit time upon peak base doping concentration is shown in Figure: 6. From the figure it is found that the base transit time increases with peak base concentration. Equation 9(a) shows that $D_n(\mu_n)$ decreases with $N_B\ (0)$. For low level of injection E(x) is given by equation 14. It shows that E(x) is independent of $N_B\ (0)$. Due to the

decreases of $D_n(\mu_n)$ the stored base charge increases resulting in an increases of $\tau_B$. For high level of injection $E(x)$ reduces in amplitude. The decreases in both the aiding electric field and the mobility contribute to the increase of $\tau_B$.

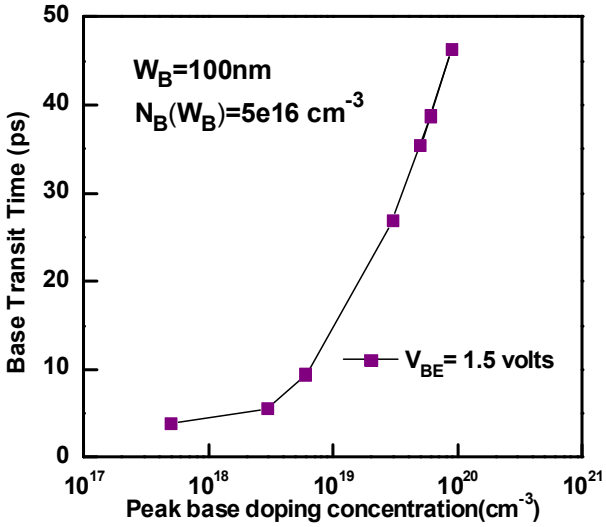


Fig. 6. Base transit time as a function of peak doping concentration with a trapezoidal shape $Al$ profile ($y_C$=0.25, $y_E$=0.1) for moderate level of injection.

Effect of change in the slope of base doping on base transit time ($\tau_B$) is also studied and the results are shown in Figure 7. From the Figure 7, it is found that the base transit time is a decreasing function of the slope of base doping for low level of injection. This is because with the increase in slope of base doping, the injected electron concentration profile become steeper

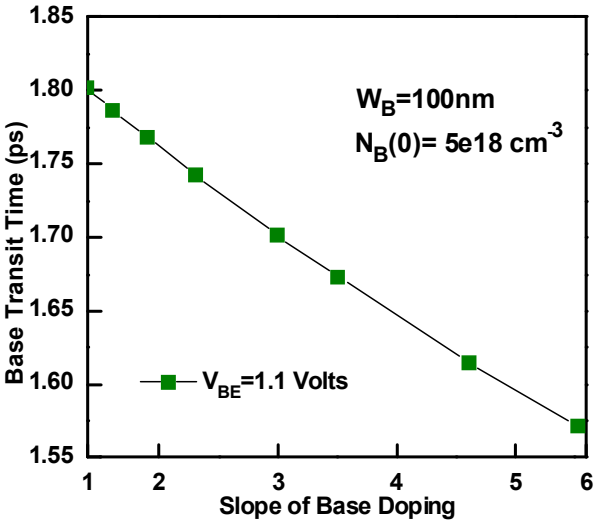


Fig. 7. Base transit time as a function of slope of base doping with a triangular shape $Al$ profile ($y_C$=0.25, $y_E$=0.01) for low level of injection.

Variation of base transit time with $Al$ concentration at the collector edge is plotted in Figure 8 and is compared with analytical model derived for base transit time of $SiGe$ HBT [9] to show that base transit time decreases in case of the proposed device. The calculated result with the present device shows similar trends as compared with published result. Here proposed device is faster than the compared device.

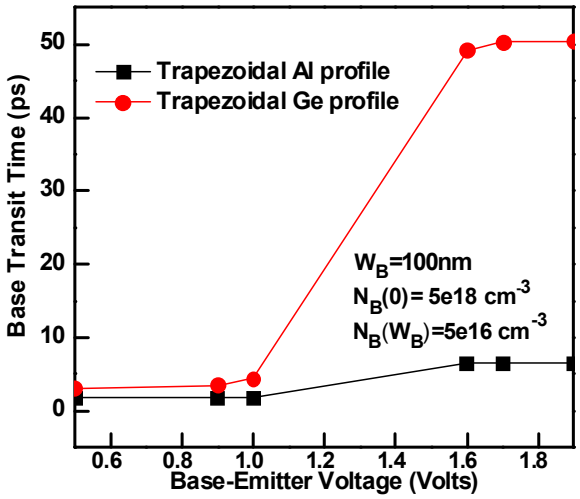


Fig. 8. Base Comparison between base transit time of $AlGaAs$ base HBT and base transit time of $SiGe$ base HBT

## IV. Conclusion

The dependency of base transit time on minority carrier injection, base width, base-emitter voltage, peak base doping concentration and slope of base doping is shown for various doping profiles (box, triangular, trapezoidal). It is observed that the base transit time increases with rise in all these factors except for slope of base doping. The base transit time shows a decreasing trend as the slope of base doping augments. A comparative analysis between $SiGe$ and $AlGaAs$ based HBT is shown where the base transit time of $AlGaAs$ HBT is found to be lower.


## Acknowledgment

The authors of this work would like to express gratitude to the corresponding Departments of their respective Institute/ University for various supports during the preparation of this manuscript.


## References


[1] Z. Xu, G. Niu, L. Luo, P. S. Chakraborty, P. Cheng, D. Thomas, and J. D. Cressler, "Cryogenic RF Small-Signal Modeling and Parameter Extraction of SiGe HBTs," IEEE Topical Meeting on Silicon Monolithic Integrated Circuits in RF Systems, SiRF'09, pp. 1-4, Jan 2009.

[2] K. Lee, D. H. Cho, K. W. Park, and B. Kim, "Improved VBIC Model for SiGe HBTs With a Unified Model of Heterojunction Barrier Effects," IEEE Tran. on Electron Devices, vol. 53(4), p. 743, 2006.

[3] F. M. Yamada, A. K. Oki, D. C. Streit, D. K. Umemoto, L. T. Tran, et al., "Reliable ICs fabricated using a production GaAs HBT process for military and commercial applications" Military Communications Conference, MILCOM '95, Conference Record, IEEE, vol. 2, pp 760 – 764, Nov 1995.

[4] S. K. Mandal, G. K. Marskole, K. S. Chari, and C. K. Maiti, "Transit time components of a SiGe-HBT at low temperature," Proc. 24th International Conference on Microelectronics, vol. 1, pp. 315-318, May 2004.

[5] Z. R. Tang, T. Kamins, and C. A. T. Salama, "Analytical and experimental characteristics of SiGe HBT with thin α-Si : H emitters," Solid-State Electron., vol. 38, pp. 1829-1834, 1995.

[6] K. H. Kwok and C. R. Selvakumar, "Profile design considerations for minimizing base transit time in SiGe HBTs for all levels of Injection before onset of Kirk effect," IEEE Tran. on Electron Devices, vol. 48, pp. 1540-1549, 2001.

[7] H. Kroemer, "Two integral relations pertaining to electron transport through a bipolar transistor with a nonuniform energy gap in the base region," Solid-State Electron., vol. 28, pp. 1101–1103, 1985.

[8] J. S. Yuan, "Effect of base profile on the base transit time of the bipolar transistor for all levels of injection," IEEE Tran. on Electron Devices, vol. 41, pp. 212-216, Feb 1994.

[9] S. M. M. Islam, M. I. B. Chowdhury, Y. Arafat, and M. Z. R. Khan, "Base Transit Time of a Heterojunction Bipolar Transistor (HBT) with Gaussian Doped Base Under High-Level of Injection," in International Conference on Devices, Circuits and Systems (ICDCS), Mar 2012.

[10] K. Suzuki, "Optimum base doping profile for minimum base transit time considering velocity saturation at base-collector junction and dependence of mobility and bandgap narrowing on doping concentration," IEEE Tran. on Electron Devices, vol. 48, pp. 2102-2107, 2001.

[11] M. Shur, Physics Of Semiconductor devices, A Prentice-Hall. Inc, 1990.

[12] S. Basu, "Analytical modelling of base transit time of SiGe HBTs including effect of temperature," International Semiconductor Conference, CAS'08, vol. 2, pp. 339-342, Oct 2008.

[13] S. T. Chang, C. W. Liu, and S. C. Lu, "Base transit time of gradedbase Si/SiGe HBTs considering recombination lifetime and velocity saturation," Solid-State Electron., vol. 48, pp. 207–215, 2004.

[14] S. M. Sze, Physics Of Semiconductor devices, A Wiley Inter science publication, 1981.

[15] V. S. Patri and M. J. Kumar, "Profile Design Considerations for minimizing base transit time in SiGe HBT's," IEEE Tran. on Electron Devices, vol. 45, pp. 1725-1731, Aug 1998.

[16] A. Zareba, L. Lukasiak, and A. Jakubowski, "Modeling of SiGe-base heterojunction bipolar transistor with gaussian doping distribution," Solid-State Electron., vol. 45, pp. 2029-2032, 2001.

[17] J. W. Slotboom and H. C. d. Graaff, "Measurement of bandgap narrowing in Si bipolar transistors," Solid-State Electron., vol. 19, pp. 857–862, 1976.

[18] T. C. Lu and J. B. Kuo, "A closed form analytical BJT forward transit time model considering bandgap narrowing effects and concentration dependent diffusion coefficients," Solid-State Electron., vol. 35, pp. 1374– 1377, 1992.

[19] H. Kroemer, "Two integral relations pertaining to electron transport through a bipolar transistor with a nonuniform energy gap in the base region," Solid-State Electron., vol. 28, pp. 1101–1103, 1985.

[20] M. M. S. Hassan and M. W. K. Nomani, "Base transit time model considering field dependent mobility for BJTs operating at high-level injection," IEEE Tran. on Electron Devices, vol. 53, pp. 2532-2539, Oct 2006.

[21] S. M. M. Islam, Y. Arafat, M. I. B. Chowdhury, M. Z. R. Khan, and M. M. S. Hassan "Base Transit Time of a Heterojunction Bipolar Transistor with Gaussian Doped Base", 6th International Conference on Electrical and Computer Engineering ICECE 2010, Dhaka, Bangladesh, December 2010.

[22] K. Suzuki, "Analytical base transit time model of uniformly-doped base bipolar transistors for high-injection regions," Solid-State Electron., vol. 36, pp. 109-110, 1993.

[23] W. Webster, "On the variation of junction-transistor current amplification factor with emitter current," Proc IRE, vol. 42(6), pp. 914-920, 1954.

[24] J. D. Cressler and G. Niu, Silicon-Germaneum Heterojunction Bipolar Transistor. Norwood, MA: Artech House, 2003.